

Giant protostellar outflows revealed by infrared imaging

Th. Stanke^{*,**}, M.J. McCaughrean, and H. Zinnecker

Astrophysikalisches Institut Potsdam (AIP), An der Sternwarte 16, 14482 Potsdam, Germany

Received 10 October 1999 / Accepted 10 December 1999

Abstract. We present new infrared data from a survey for embedded protostellar jets in the Orion A cloud. This survey makes use of the S(1) $v = 1-0$ line of molecular hydrogen at $\lambda = 2.12 \mu\text{m}$ to search for infrared jets deep inside the cloud and thus hidden from view at optical wavelengths. We present data on the three flows associated with the Herbig-Haro objects HH 43/38 & HH 64, HH 65, and the L1641-N giant flow. HH 43, HH 38 and HH 64 are part of one H₂ flow extending over at least 1.4 pc. We identify a deeply embedded 1.3 mm and IRAS source (HH 43 MMS1 = IRAS 05355–0709C) as the likely driving source, while the infrared source previously assumed to drive HH 43/38 (HH 43-IRS1 = IRAS 05357–0710) is seen to drive a smaller jet. The morphology of HH 43-IRS1 suggests that it is a star+disk system seen close to edge-on. We identify another large H₂ flow apparently comprising the L1641-S3 CO outflow and the redshifted lobe of the L1641-S CO outflow containing HH 65. This flow extends over at least 2.6 pc and appears strongly curved. It is driven by L1641-S3 IRS, a deeply embedded 1.3 mm and IRAS source (L1641-S3 MMS1 = IRAS 05375–0731). Finally, we have found some additional large H₂ features to the east of V 380 Ori and the HH 1/2 system, which probably outline another part of the L1641-N outflow. The molecular flow MB 20/21, which extends to the south from V 380 Ori, also appears to be a part of the L1641-N outflow.

Key words: ISM: jets and outflows – stars: formation – stars: circumstellar matter – infrared: ISM: lines and bands

1. Introduction

Star formation is known to be intimately connected with outflow activity, especially when the star is in its main accretion phase, still deeply embedded in its parent cloud (e.g. Bontemps et al. 1996). Many low-mass young stellar objects are found to drive well-collimated jets. Interestingly, the length-scales of these jets

have increased with advances in detector technology, namely bigger imaging arrays. It now seems that flows from low-mass stars extending over several parsecs are no great exception (e.g. Bally & Devine 1994, 1997; Devine et al. 1997; Eisloffel & Mundt 1997; Reipurth et al. 1997, 1998; Stanke et al. 1999); however, the great majority of them have been found at optical wavelengths.

In this paper we demonstrate that infrared imaging is also capable of revealing large scale flows. This is complementary progress, since infrared imaging is a much more efficient way of finding jets deep in molecular clouds and interacting with the clouds, as these are hidden from view at optical wavelengths (e.g. the infrared jets HH 211; McCaughrean et al. 1994; and HH 212; Zinnecker et al. 1998). Only a combination of infrared and optical imaging can fully reveal the true number of jets in a cloud and thus enable us to address questions concerning the role of outflows from young stars for the evolution of a cloud, e.g. in terms of momentum-injection to stabilize the cloud against collapse.

The data presented here are part of an infrared survey for embedded jets in the Orion A cloud. The full survey will cover an area of about 1 square degree with a sensitivity comparable to that of previous infrared observations of individual protostellar jets. Initial results from the survey were published by Stanke et al. (1998, Paper I in the following). The new results presented here confirm that infrared imaging is an efficient way to search large areas for embedded flows hidden from view at optical wavelengths, but which are bright in H₂ emission in the near-infrared.

2. Observations

The infrared data presented here were obtained during several observing runs (Jan. 10-11 1998, Oct. 23-26 1998, Dec. 5 1998) using the Omega Prime wide-field near-IR camera (Bizenberger et al. 1998; McCaughrean et al., in prep.) on the Calar Alto 3.5 m telescope. The camera uses a 1024×1024 pixel HgCdTe array: at 0.4 arcsec per pixel, the field-of-view is 6.7 arcmin×6.7 arcmin. Images were taken through a 1 % filter centred on the $v = 1-0$ S(1) line of H₂ at 2.12 μm and a broad-band K' filter (1.944–2.292 μm) in order to discriminate line and continuum sources. The images presented here are ex-

Send offprint requests to: T. Stanke (tstanke@mpifr-bonn.mpg.de)

* Visiting Astronomer, German-Spanish Astronomical Centre, Calar Alto operated by the Max-Planck-Institute for Astronomy, Heidelberg, jointly with the Spanish National Commission for Astronomy

** Now at Max-Planck-Institut für Radioastronomie Bonn, Auf dem Hügel 69, 53121 Bonn, Germany

cerpts of larger mosaics, each of them a combination of 36 overlapping images. In the $2.12\ \mu\text{m}$ filter, the net integration time was 10 min in the central part of each mosaic and 5 min at its edges; at K' , the corresponding integration times were 1 min and 30 sec. We reach a 5σ limiting H_2 surface brightness of $\sim 10^{-18}\ \text{W m}^{-2}\ \text{arcsec}^{-2}$ ($K' \sim 17$ for continuum point sources). Standard data reduction techniques were used to sky subtract, flat field, and mosaic the data (McCaughrean et al. 1994).

The data discussed in this paper are part of a much larger survey in Orion A split into a number of overlapping fields. We only assign designations to those H_2 features which are part of the outflows discussed here. We adopt a nomenclature similar to that used in Paper I, with an additional digit indicating the survey field. For example, SMZ 7-10 means H_2 feature number 10 in survey field 7. A complete catalogue of all features found during our survey is deferred to a future paper.

Millimetre continuum maps at 1.3 mm were taken of several of the most interesting new H_2 sources during an observing run in February 1999, using the MPIfR 37 channel bolometer array on the IRAM 30 m telescope on Pico Veleta. The details of these observations as well as the complete results will be discussed elsewhere; here we will only present data related to the flows discussed in this paper.

3. The HH 43/38 outflow

3.1. Previous studies

HH 43 and HH 38 were discovered via optical photography by Haro (1953; see Herbig 1974). CCD images of these objects were presented by Strom et al. (1986) and Eislöffel & Mundt (1997), the latter discovering another feature, HH 43X, north-west of HH 43. Infrared studies of H_2 line emission from HH 43 have been reported in several papers (Schwartz et al. 1987, 1988; Zinnecker et al. 1989; Gredel 1994; Schwartz & Greene 1999). An optically invisible infrared source (HH 43-IRS1, IRAS 05357–0710) north-west of HH 43 was considered as the source of the HH 43/38 system (Cohen & Schwartz 1983, 1987; Reipurth & Aspin 1997). Cohen et al. (1984, 1985) presented far-infrared (47–130 μm) measurements of this source, showing it to be a cool low-luminosity object. At near-infrared wavelengths, the source was resolved into a double star with some associated nebosity (Gredel 1994; Moneti & Reipurth 1995). Casali (1995) measured the K-band polarisation of the source as 3.78% at a position angle of 46 degrees.

Searching for a molecular outflow associated with the HH objects, Edwards & Snell (1983, 1984) found no evidence for well-ordered supersonic molecular motion there, and while Morgan & Bally (1991) observed some evidence for high-velocity material at the position of IRAS 05357–0710, they later regarded this not to be a molecular outflow in a follow-up paper (Morgan et al. 1991).

HH 64 was found by Reipurth & Graham (1988). Cohen (1990) found a very red IRAS source (IRAS 05355–0709C) close to this HH-object, which they assumed to be its driving source. The region was searched for CS (1–0) emission by

Table 1. Positions of the H_2 features discussed in the text. The features are located in survey fields 6, 7, and 9.

Name	RA	Dec	d ^a		Note
	J2000.0		arcmin	pc	
SMZ 6-2	5 36 30.6	−6 40 00	18.1	2.4	
6-4A	5 36 32.0	−6 42 28	20.5	2.7	
6-4B	5 36 33.6	−6 44 12	22.3	2.9	
6-4C	5 36 35.2	−6 45 40	23.7	3.1	
6-16	5 36 33.1	−6 53 25	31.3	4.1	
7-5	5 37 47.0	−7 05 22	3.0	0.39	HH 64
7-6	5 37 51.5	−7 06 08	1.5	0.19	
7-7	5 38 01.0	−7 07 39	1.1	0.15	
7-8	5 38 03.9	−7 07 47	1.1	0.15	
7-9	5 38 05.5	−7 08 30	2.5	0.32	HH 43X
7-10 ^b	5 38 10.8	−7 09 25	4.2	0.55	HH 43
7-14	5 38 21.8	−7 11 36	7.6	1.0	HH 38
9-3A	5 40 25.8	−7 22 14	11.1	1.4	
9-3B	5 40 23.4	−7 22 48	10.2	1.3	
9-4A	5 40 43.0	−7 23 29	13.7	1.8	
9-5A	5 40 23.9	−7 24 29	9.2	1.2	
9-6A	5 40 15.3	−7 24 25	7.6	1.0	
9-11A	5 39 53.3	−7 30 57	0.74	0.1	
9-12A	5 39 45.8	−7 34 44	5.0	0.65	
9-12B	5 39 42.2	−7 32 51	4.1	0.53	
9-13A	5 39 49.9	−7 33 54	3.7	0.48	
9-14A	5 39 40.6	−7 35 26	6.2	0.8	
9-15	5 39 46.3	−7 36 52	6.9	0.9	

^a Separation from the driving source measured in arcmin and in pc (projected separation assuming a distance to the Orion star forming region of 450 pc)

^b Knot B2, see Schwartz et al. 1988

Tatematsu et al. (1993) and Morata et al. (1997). Tatematsu et al. found two cores which appear to be at the positions of the IRAS sources: their core #98 corresponds to IRAS 05357–0710, and core #97 to IRAS 05355–0709C. Anglada et al. (1989) observed an ammonia condensation at the position of the latter core and suggested that the source responsible for the excitation of HH 64 as well as HH 43/38 might be embedded in this condensation. Below we show that this hypothesis was correct.

3.2. New observational results

Fig. 1 shows the region around HH 43/38 and to their north-west as we have imaged it. A long chain of H_2 features is clearly identified, delineating a well collimated jet. HH 38 (SMZ 7-14), HH 43 (SMZ 7-10), and HH 43X (SMZ 7-9) are seen to be part of the south-eastern lobe of this jet. A gap is evident between features SMZ 7-7 and SMZ 7-6. The latter features, along with HH 43X and HH 64, are seen to form two pairs lying roughly symmetrically around the middle of this gap. No further H_2 features (besides possibly some very faint traces of emission) are found to the north-west of HH 64 out to a distance of ~ 8 arcmin from the middle of the gap, although it should be noted that the outermost part of the image is from data taken under rather bad weather conditions, leading to a nominally poorer detection limit; nevertheless, features with a H_2 brightness comparable to

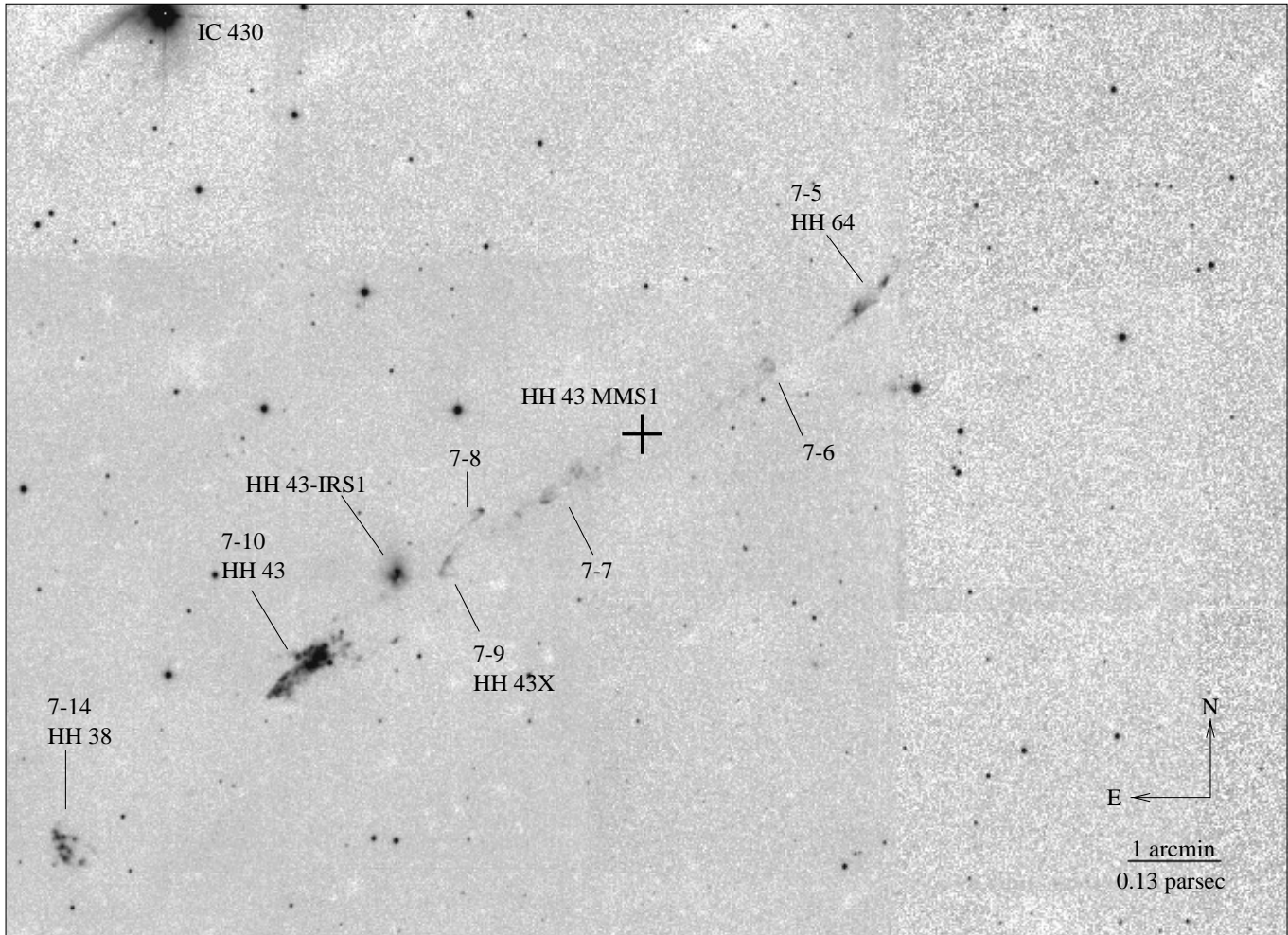


Fig. 1. 2.12 μm image (not continuum subtracted) of the HH 43/38 region. The image size is $\sim 14 \text{ arcmin} \times 10 \text{ arcmin}$ ($1.8 \text{ pc} \times 1.3 \text{ pc}$). H_2 features are labeled with their SMZ numbers. The cross marks the position of HH 43 MMS1 ($\alpha = 5^{\text{h}}37^{\text{m}}57.5^{\text{s}}$, $\delta = -7^{\circ}07'00''$ (J2000)), which apparently drives the jet outlined by SMZ 7-5, 7-6, 7-7, 7-9, 7-10, and 7-14. A certain symmetry of the H_2 features is seen around MMS1, which however breaks down at larger distances: HH 43 and HH 38 are without similar brightness counterparts on the other side of the driving source. The apparent symmetry and morphology in the knots led us to suspect that the driving source was located somewhere between SMZ 7-6 and 7-7, as confirmed by the subsequent discovery of MMS1. HH 43-IRS1 is unrelated to the large flow, but is seen to drive a smaller jet as indicated by SMZ 7-8, a bow-shock like H_2 feature that opens back towards HH 43-IRS1, not MMS1.

HH 43 can safely be excluded. We do not detect any continuum emission in the gap between SMZ 7-6 and 7-7 to a limiting magnitude of about $K=17.5$ (3σ for a point source).

To the north-west of HH 43X we identify a cometary H_2 feature (SMZ 7-8, see Fig. 2) with a bright head to the north-west and a tail to the south-east, which is clearly displaced from the axis of the large flow. The tail points back to HH 43-IRS1, which is resolved into the components previously reported by Gredel (1994) and Moneti & Reipurth (1995). The diffuse nebulosity consists of two roughly symmetric lobes separated by a dark lane, which is oriented at an angle of ~ 45 degrees east of north. The fainter star is located slightly displaced from the centre of symmetry of the nebulosity (~ 0.6 – 0.9 arcsec to the north-west). The dark lane is about 2.5 arcsec wide and at least 4 arcsec long, corresponding to about 1100 AU and 1800 AU respectively at a distance of 450 pc .

We examined HIRES-processed IRAS maps of the area around HH 43, as shown in Fig. 3. HH 43-IRS1 (IRAS 05357–0710) is detected at all four IRAS wavelengths. Cohen (1990) found an additional source (IRAS 05355–0709C) on the coadded IRAS images, which is not in the Point Source Catalog, but is clearly seen in the $60 \mu\text{m}$ and $100 \mu\text{m}$ HIRES maps. From the $60 \mu\text{m}$ map (with 10 iterations of HIRES processing) we find this source to be located at $\alpha = 5^{\text{h}}37^{\text{m}}57.8^{\text{s}}$, $\delta = -7^{\circ}07'03''$ (J2000), which is about 30 arcsec north-east of the position given by Cohen (1990). However, the positional accuracy (as defined by the deconvolution) is probably not better than a few pixels, that is about 30 arcsec . IRAS 05355–0709C is fainter than IRAS 05357–0710 at $60 \mu\text{m}$, but brighter at $100 \mu\text{m}$, consistent with the fluxes given for these sources by Cohen (1990) and Cohen & Schwartz (1987).

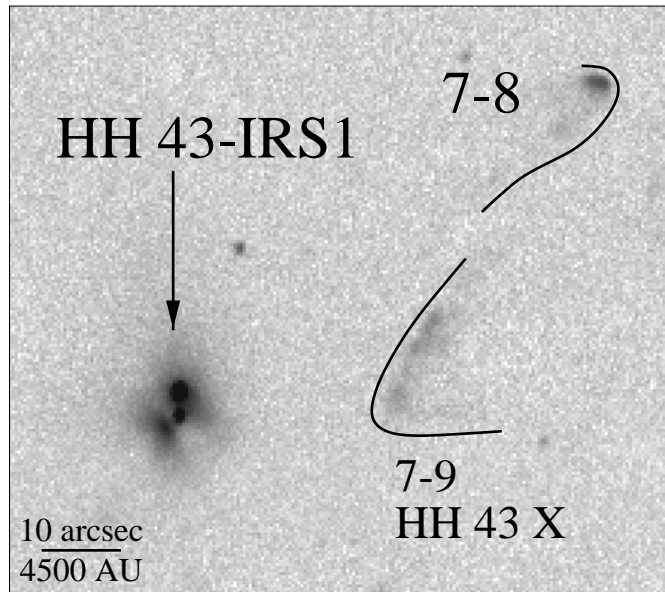


Fig. 2. $2.12\ \mu\text{m}$ image (not continuum subtracted) of the area around HH 43-IRS1 (IRAS 05357–0710). SMZ 7-8 consists of a bright knot with a faint diffuse tail extending south-east towards HH 43-IRS1. HH 43-IRS1 itself is resolved into two stellar sources plus a bipolar continuum nebula intersected by a dark lane. The fainter star, located within the dark lane, appears to be surrounded by an almost edge on disklike structure causing the dark lane, and a diffuse envelope causing the bipolar reflection nebulosity. SMZ 7-8 seems to mark a bow shock caused by a jet from the star+disk system. The line connecting the star and SMZ 7-8 is nearly perpendicular to the dark lane, suggesting that the jet is roughly perpendicular to the disk plane.

In addition, a strong compact 1.3 mm source was found at $\alpha = 5^{\text{h}}37^{\text{m}}57.^{\text{s}}5$, $\delta = -7^{\circ}07'00''$ (J2000; positional accuracy ~ 3 arcsec) with a flux of about 600 mJy in an 11 arcsec beam. This source is henceforth referred to as HH 43 MMS1. A 4 arcmin \times 4.6 arcmin section of the 1.3 mm map is shown in Fig. 4 as a contour plot overlaid on the corresponding $2.12\ \mu\text{m}$ infrared image. Some 32 arcsec south and 20 arcsec west of HH 43 MMS1 there is an east-west elongated ridge of emission, which we label HH 43 MMS2. Surrounding both features there appears to be substantial extended emission out to about 30 arcsec north-east and 100 arcsec to the west and south-west of HH 43 MMS1. No significant emission was detected from HH 43-IRS1, a result which is consistent with our detection limit of ~ 50 mJy and the 1.3 mm flux of 47 ± 14 mJy measured by Reipurth et al. (1993). The position of HH 43 MMS1 coincides with that of IRAS 05355–0709C to within a few arcseconds, and thus it is very likely the same source that is seen at $60\ \mu\text{m}$, $100\ \mu\text{m}$, and 1.3 mm.

3.3. Discussion

The new near-infrared data clearly show that the HH-objects 38, 43, and 64 are part of a single well-collimated flow. It extends over at least 11 arcmin in projection (from HH 38 to HH 64 only) equivalent to 1.4 pc at a distance of 450 pc. This projected length

is probably close to the true length of the flow, since infrared spectroscopy of HH 43 indicates that the flow lies close to the plane of the sky (e.g. Schwartz & Greene 1999).

The driving source of this flow appears to be the newly discovered 1.3 mm object HH 43 MMS1, which is associated with the cold IRAS source 05355–0709C, embedded in a dense NH_3/CS core (Anglada et al. 1989; Morata et al. 1997; Tatematsu et al. 1993), and appears to be a very good candidate for a Class 0 protostar (see Fig. 5). It seems reasonable to assume that the flow is intrinsically fully symmetric and extends out to similar distances on both sides of its source with a total length of ~ 2 pc (the distance from the source to HH 38 is about 1 pc). Indeed, some very faint traces of emission might be present in our low S/N data north-west of HH 64, but this has to be confirmed. A similar break in symmetry is also observed in HH 212, the prototypical symmetric H_2 jet (Zinnecker et al. 1998), where the outermost bow shock is only visible in one jet lobe.

Identifying HH 43 MMS1 as the driving source also removes the difficulties in explaining the morphology of some features (see e.g. Eislöffel & Mundt 1997): the south-eastern part of HH 43 as well as the bow-shock like HH 43X clearly do not point back towards HH 43-IRS1, but towards HH 43 MMS1. Thus HH 43-IRS1 seems to be unrelated to HH 43 and the associated infrared jet. HH 43 MMS1 is obviously deeply embedded, since it is only seen at the longest IRAS and millimetre wavelengths and is completely invisible in our K-band images. It is likely a Class 0 type object, as is suggested by the model SED (Fig. 5), which yields a ratio of $L_{\text{bol}}/L_{\text{submm}}$ of only 11 (note that the high-frequency fit in the two component curve in Fig. 5 is only constrained by upper limits, the derived $L_{\text{bol}}/L_{\text{submm}}$ of 11 thus is in fact an upper limit). HH 43 MMS1 thus easily fulfills the criterion for a classification as a Class 0 object ($L_{\text{bol}}/L_{\text{submm}} < 200$) suggested by André et al. (1993). Additional (sub)millimetre continuum observations are needed to further constrain the SED of HH 43 MMS1 and to estimate its evolutionary stage.

The K-band morphology of HH 43-IRS1 suggests that the southern star is surrounded by a disk-like structure or a flattened envelope which is seen close to edge on, and a tenuous, more spherically symmetric envelope. The star appears within the dark lane, located close to its north-western edge. This suggests that the north-western part of the disk is slightly tilted towards the observer. The disk is seen at a position angle of ~ 45 degrees, in excellent agreement with the polarization angle derived by Casali (1995), assuming that light scattered in a tenuous envelope above a disk-like dust configuration will yield a polarization angle parallel to the disk plane (e.g. Elsässer & Staude 1978; Fischer et al. 1994, 1996). Since the disk is seen close to edge-on, the star suffers substantial extinction, which leads to its disappearance at shorter wavelengths (see Moneti & Reipurth 1995). The star to the north, which is the brighter component of the system in the K-band, also disappears at shorter wavelengths and is thus heavily extinguished. It is probably located behind the star+disk system; whether it is physically related to the system is not clear. We cannot exclude the possibility that it is a background star, but since there is a dense cloud core

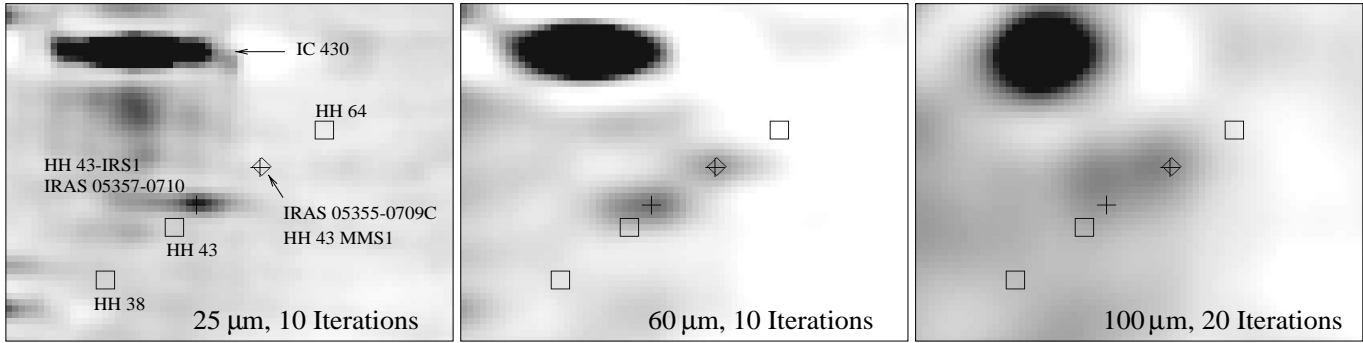


Fig. 3. HIRIS-processed IRAS images of the HH 43 region (pixel size is 15 arcsec, field size is $17.5 \text{ arcmin} \times 13.75 \text{ arcmin}$). The positions of the HH-objects 38, 43, and 64 (from left to right) are indicated as squares, crosses mark the positions of the IRAS sources 05357–0710 (HH 43-IRS1, previously assumed to be the driving source of the HH 43/38 flow; see Cohen & Schwartz 1983, 1987) and 05355–0709C. In addition, the position of HH 43 MMS1 is marked by a diamond. The positional accuracy for IRAS 05355–0709C is probably limited by the deconvolution process and of the order of ~ 2 pixels, corresponding to about 30 arcsec. Within these errors, HH 43 MMS1 and IRAS 05355–0709C are coincident.

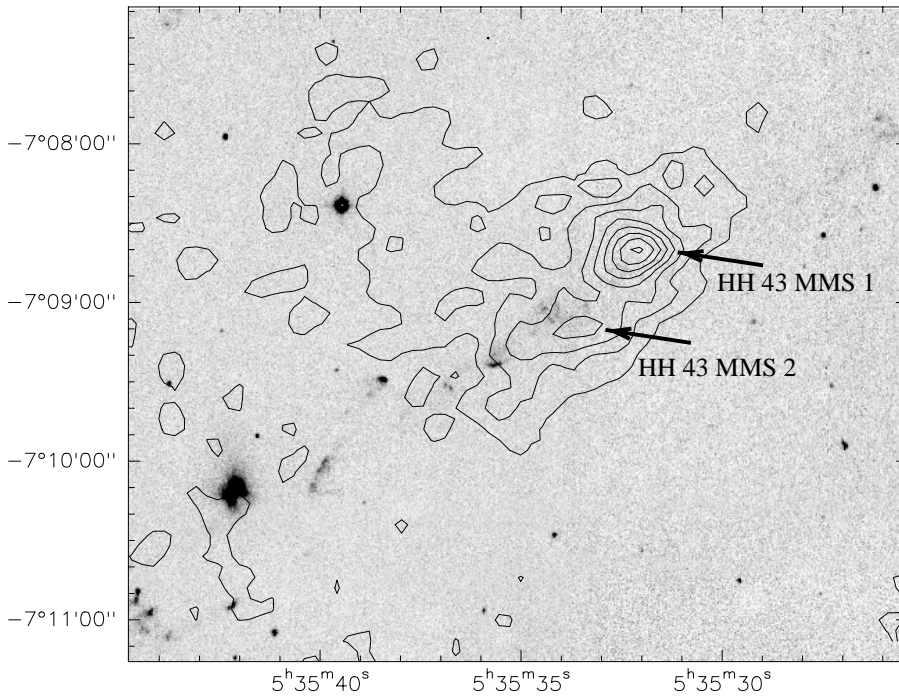


Fig. 4. This image shows a contour plot of a 1.3 mm map of the region around the HH 43/38 outflow source (resolution ~ 15 arcsec), superimposed on a narrow band $2.12 \mu\text{m}$ image. The contours start at a level of 20 mJy and increase in steps of 20 mJy. Positions are in B1950.

associated with HH 43-IRS1, it might well be another young star embedded in the same core. The dust lane separating the lobes of the reflection nebula in HH 43-IRS1 seems to be much bigger than those observed in YSOs in the Taurus star forming region (Padgett et al. 1999) and the Orion Nebula silhouette disks (McCaughrean & O’Dell 1996; McCaughrean et al. 1998).

The connecting line between SMZ 7-8 to the north-west and the star in the dark lane is at 85 degrees with respect to the dark lane, consistent with the usual finding that jets are perpendicular to the disks of their driving sources. The morphology of SMZ 7-8 is suggestive of a bow shock like structure heading away from the disk+star system. We thus regard the disk+star system as the source of a second jet which includes knot SMZ 7-8 (see Fig. 2), independent of the large HH 38/43/64 flow from HH 43 MMS1. There is no conclusive evidence for a counter jet in this system, although if we reflect the north-

western bow symmetrically about the disk, a putative counter-jet would lie at the northern edge of HH 43, making it hard to see against this bright feature. Furthermore, the suggested inclination of the disk also implies that the north-western part of the jet is the blueshifted lobe, whereas the counter-lobe would be redshifted, running into the cloud, and thus possibly heavily obscured.

4. The L1641-S and L1641-S3 flow

4.1. Previous studies

IRAS 05380–0728 is located about 10 arcmin to the south and 34 arcmin to the east of the HH 43 region and is one of the more luminous young stellar objects in the L1641 cloud ($\sim 250\text{--}370 L_{\odot}$; Reipurth & Bally 1986; Cohen 1990), probably a low-

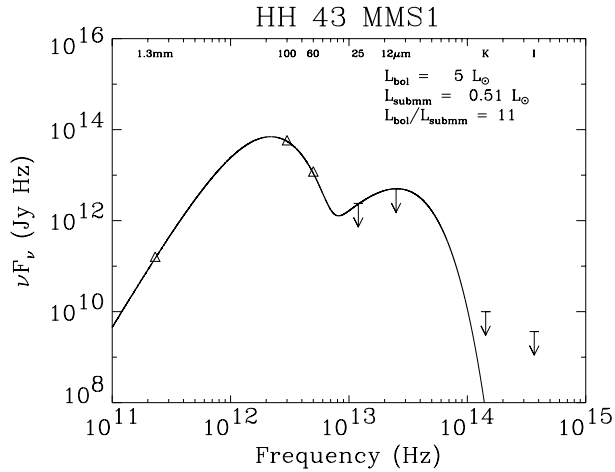


Fig. 5. Spectral energy distribution of the driving source of the HH 43 jet. 1.3 mm, K-, and I-band photometry/upper limits are derived from our own data, and IRAS photometry is taken from Cohen (1990). In addition to the data points we show the curve which was used to derive the total luminosity L_{bol} and the submillimetre luminosity L_{submm} of the source based on “bluebody” curves (see Dent et al. 1998) with $F_{\nu} \propto B_{\nu}(T) \times (1 - e^{-\tau_{\nu}})$ and $\tau_{\nu} \propto (\nu/\nu_0)^{\beta}$. We did not attempt to derive the circumstellar dust mass or dust properties: the curves were only used to get an estimate of $L_{\text{bol}}/L_{\text{submm}}$ by integrating over F_{ν} from $\lambda = 3 \text{ mm}$ to $300 \mu\text{m}$ (L_{submm}) and to $10 \mu\text{m}$ (L_{bol}). According to the criterion for a classification as a Class 0 source ($L_{\text{bol}}/L_{\text{submm}} < 200$) suggested by André et al. (1993), HH 43 MMS1 qualifies as Class 0 protostar.

to intermediate-mass star which may have undergone an FU Orionis type outburst (Strom & Strom 1993). Fig. 6 shows a $2.12 \mu\text{m}$ image of the area around this source and its associated reflection nebulosities Re 50 and Re 50 N (Reipurth 1985; Strom et al. 1989; Heyer et al. 1990; Casali 1991; Chen & Tokunaga 1994; Hodapp 1994; Casali 1995; Colomé et al. 1996; Reipurth & Aspin 1997). Reipurth & Bally (1986) and Fukui et al. (1986) independently discovered a bipolar high velocity molecular gas flow apparently from IRAS 05380–0728, the so-called L1641-S outflow. Further mapping of the high velocity gas in this flow presented by Morgan et al. (1991, flow MB 40) showed that the northern redshifted lobe of the flow describes a long curve to the north and west of the IRAS source position (see contour-overlay on the infrared image in Fig. 6). HH 65 is located within this lobe (Reipurth & Graham 1988). Far-infrared and submillimetre measurements for IRAS 05380–0728 have been presented by Reipurth et al. (1993), Colomé et al. (1996), Chini et al. (1997), Zavagno et al. (1997), and Di Francesco et al. (1998); see also Cohen (1990). Morgan et al. (1990) found two radio continuum sources in the region surrounding Re 50 N; one is close to the IRAS and $2 \mu\text{m}$ source position of the central source of the Re 50 N nebulosity, while the second is displaced by 50 arcsec to the west. There is no NH_3 core associated with this second source (Wouterloot et al. 1988, 1989).

Another IRAS source (IRAS 05375–0731) is found about 3 arcmin south and 7.9 arcmin west of IRAS 05380–0728. It is

associated with the molecular outflow L1641-S3 (Fukui 1988; Fukui et al. 1989). The distribution of high velocity molecular material around IRAS 05375–0731 has been mapped by Wilking et al. (1990) and Morgan et al. (1991, flow MB 41, see overlay of CO contours on the infrared image in Fig. 6). While Morgan et al. (1991) found a bipolar distribution, Wilking et al. (1990) found a superposition of blue- and redshifted gas, possibly indicating a flow lying close to the plane of the sky. Near-infrared images (Chen & Tokunaga 1994; Hodapp 1994; Strom et al. 1989) revealed a small group of rather faint stars close to the IRAS source position; it is not entirely clear if any of them are the direct counterpart to the IRAS source, but the reddest one was labeled as L1641-S3 IRS by Chen & Tokunaga. Also associated with this region are a radio continuum source (Morgan et al. 1990) and a water maser (Wouterloot & Walmsley 1986), although the latter was not redetected in a later study by Felli et al. (1992). The source has been detected by Price et al. (1983) as FIRSSE 101 in the far-infrared; further measurements in the far-infrared/submillimetre range are presented by Zavagno et al. (1997). Finally, there is an NH_3 core associated with IRAS 05375–0731 (Wouterloot et al. 1988, 1989).

4.2. New observational results

Fig. 6 shows a $17 \text{ arcmin} \times 17 \text{ arcmin}$ $2.12 \mu\text{m}$ narrow band image of the L1641-S/L1641-S3 area, while Fig. 7 shows the same region after continuum subtraction. The main feature is a large system of H_2 knots and filaments to the north of Re 50 labelled SMZ 9-4, SMZ 9-5, and SMZ 9-6. HH 65 is seen to be part of the much bigger feature SMZ 9-6, including a bright, smoothly curving filamentary structure SMZ 9-6A to the north-west of HH 65. Further east, a number of fainter, more diffuse features (together labeled SMZ 9-5) define a curving path which first heads eastwards, then turns slightly to the south, and then more to the north again. Finally it ends in a multiple filamentary structure (SMZ 9-4), with the filaments curving in a similar way to the filament SMZ 9-6A. In the south-west corner of the image we find several faint, diffuse H_2 structures (SMZ 9-11, SMZ 9-12, SMZ 9-13, SMZ 9-14, and SMZ 9-15). Further faint structures are also visible to the west and south of Re 50 N. Finally, a few more H_2 features (SMZ 9-3) are found north-east and north-west of the brightest H_2 filament. The near-infrared source designated as L1641-S3 IRS appears extended in our images and is located at $\alpha = 5^{\text{h}}39^{\text{m}}55^{\text{s}}.8$, $\delta = -7^{\circ}30'28''$ (J2000).

Fig. 8 shows an overlay of a contour plot of a 1.3 mm map of the L1641-S3 outflow source region on the $2.12 \mu\text{m}$ image. A strong pointlike 1.3 mm source is found at $\alpha = 5^{\text{h}}39^{\text{m}}55^{\text{s}}.9$, $\delta = -7^{\circ}30'28''$ (J2000), coincident with L1641-S3 IRS within the positional errors of the 1.3 mm maps ($\sim 3 \text{ arcsec}$). A second fainter millimetre continuum source is found 20 arcsec to the west and 55 arcsec to the north. Further north, at about $\alpha = 5^{\text{h}}39^{\text{m}}57^{\text{s}}$, $\delta = -7^{\circ}26'50''$ (J2000), we find a large patch of extended emission (size about $4 \text{ arcmin} \times 2 \text{ arcmin}$). There appears to be some low-level extended emission 4 arcmin west of L1641-S3 MMS1 as well.

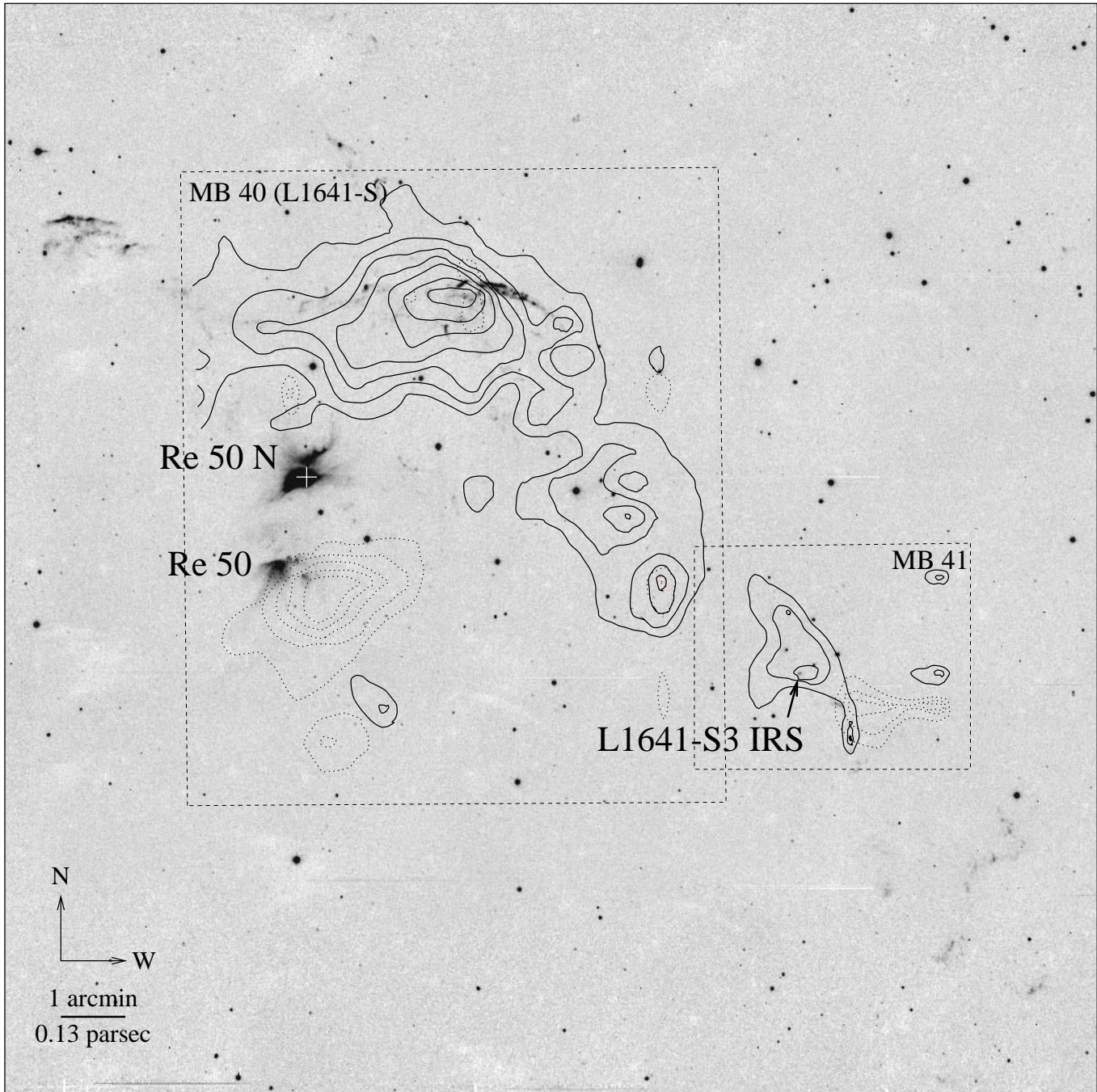


Fig. 6. $2.12\ \mu\text{m}$ image (not continuum subtracted) of the L1641-S and L1641-S3 region. The image size is $\sim 17\ \text{arcmin} \times 17\ \text{arcmin}$ ($\sim 2.2\ \text{pc} \times 2.2\ \text{pc}$). The contours show the distribution of high-velocity CO (adapted from Morgan et al. 1991). Solid lines indicate redshifted, dotted lines blueshifted gas. The dashed lines mark the boundaries of the maps presented by Morgan et al.; the large eastern square surrounds the area of flow MB 40, the smaller rectangular piece to the west the area of flow MB 41. The position of IRAS 05380–0728 is marked by a white cross; L1641-S3 IRS is coincident with IRAS 05375–0731 within the errors.

4.3. Discussion

As in the case of the HH 43 flow system, our new sensitive wide field infrared data suggest a revised picture for the L1641-S and L1641-S3 region. The dominating outflow seems not to be driven by the luminous source associated with Re 50 N, but rather by L1641-S3 IRS (IRAS 05375–0731). This flow in-

cludes the CO outflows L1641-S3 and the redshifted lobe of L1641-S, and is traced by infrared H_2 emission over much of its length.

The H_2 features SMZ 9-11 to 9-15 in the blueshifted lobe of L1641-S3 (which has not been mapped in CO), suggest a wide opening angle (~ 40 degrees) of the flow on this side. The

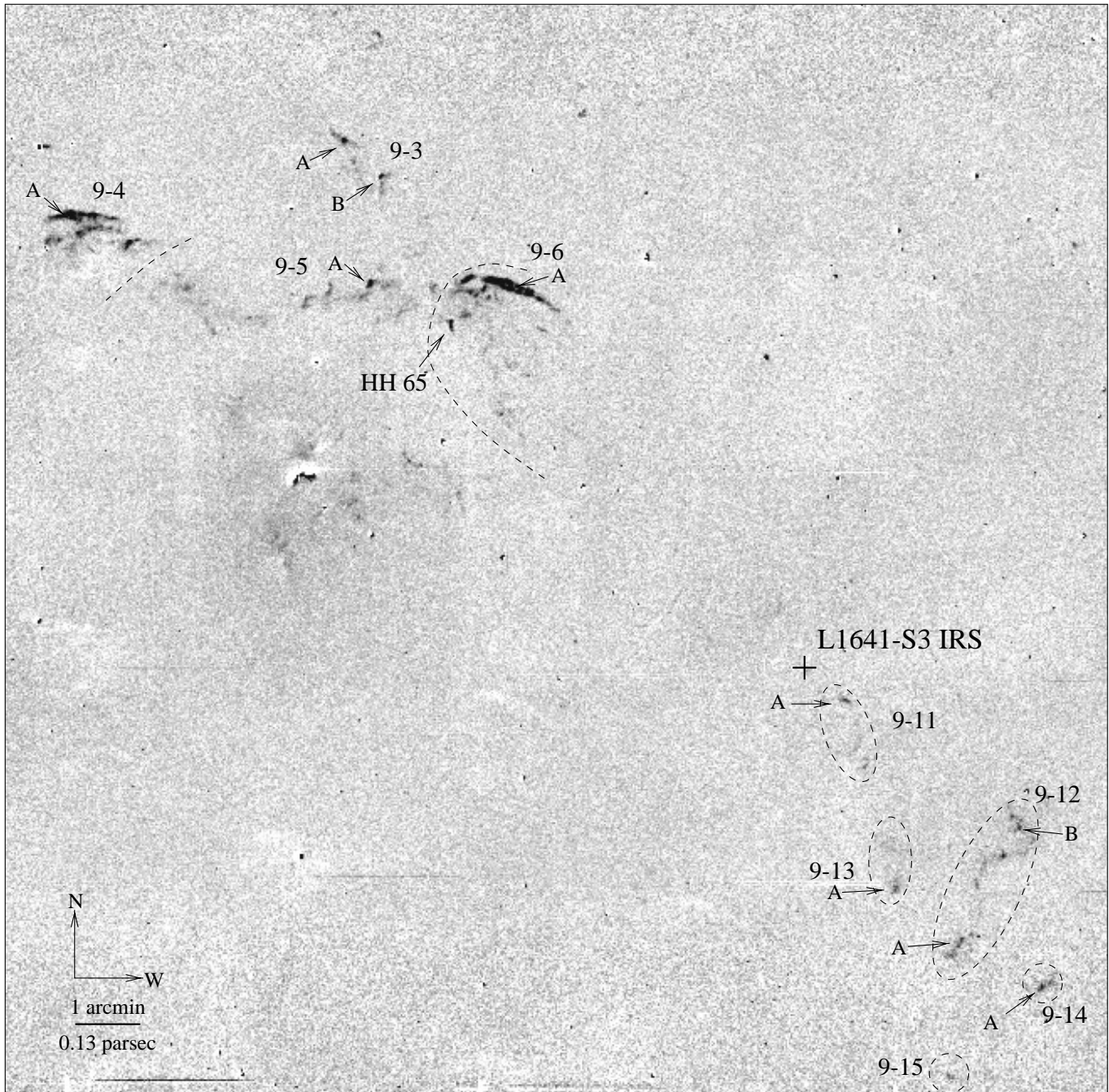


Fig. 7. Continuum subtracted image of the same area as in Fig. 6. H₂ features related to the suggested flow from L1641-S3 IRS = L1641-S3 MMS1 (as discussed in the body of the paper) are labeled with their SMZ numbers. In addition, some more H₂ features are found around Re 50 N and at the northern edge of the image. The cross marks the position of L1641-S3 IRS.

redshifted lobe is defined by the redshifted molecular gas of the L1641-S3 and L1641-S flows (MB 41 and MB 40). As is seen in Fig. 6, these CO lobes appear to trace a single outflow lobe when placed alongside each other. The flow shows very strong bending. Close to the source, it is oriented at a position angle of about 60 degrees, then turns north to a position angle of about 30 degrees, then at about the location of HH 65 and the bright H₂ filament SMZ 9-6A (and also the peak in the redshifted CO emission), it bends strongly to an eastward flow direction at

SMZ 9-5, before finally turning back north to roughly its original position angle of 60 degrees at SMZ 9-4. This behaviour is reminiscent of the wiggling of the HH 46/47 jet (e.g. Heathcote et al. 1996), albeit on a much larger scale; for example, the bright curving H₂ filaments in SMZ 9-6 mimic the H α wisps found in HH 46/47 at the positions of apparent bends in the jet. Heathcote et al. suggested that the gas does not really flow along the channel defined by the Herbig-Haro emission, but ballistically along the original direction, with the wiggles reflecting

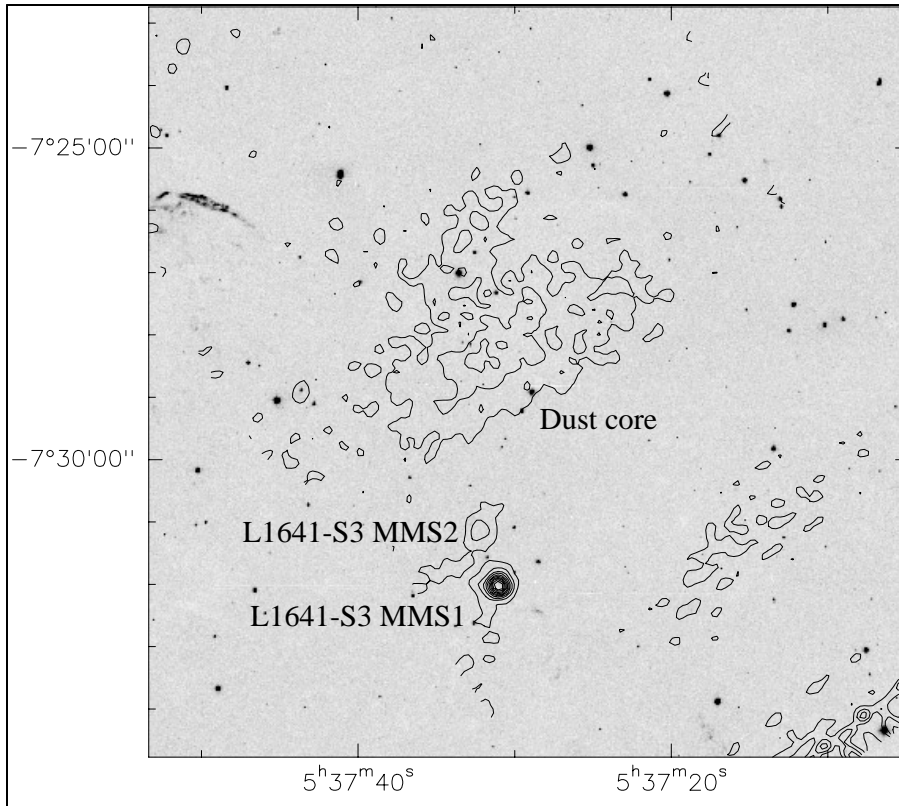


Fig. 8. This image shows a 1.3 mm contour plot of the region around the L1641-S3 outflow source, superimposed on our narrow band 2.12 μm image. The contours start at a level of 25 mJy and increase in steps of 30 mJy. The lower left and the upper right corner were not covered by our mm-mapping. The features in the lower right corner are noise peaks. Positions are in B1950.

changes in the direction of ejection of the gas at the source. This is probably the case here as well. The direction of the flow at its end and close to the source appear to be the same, thus it might be delineating one period, assuming that the changes are periodic, e.g. caused by a companion star. Assuming a typical tangential flow velocity of about 200 km/s, the distance from the source to the outermost part of the flow (1.8 pc) translates to a period of about 9000 yr. If we assume that the wiggle of the jet is simply caused by periodic changes of the source position in a binary orbit (see e.g. Fendt & Zinnecker 1998), this period would imply a separation of the binary components of order 1000 AU or a few arcsec at the distance to Orion. However, the apparent widening of both outflow lobes with distance from the source and the large amplitude of the wiggles cannot be explained by simply shifting around the outflow source in any reasonable binary orbit, and rather suggest a precessing outflow than just a moving source. A precessing jet would be caused by a precessing disk, which would be expected in a binary system with non-coplanar disk and orbital planes. Following the arguments given by Terquem et al. (1999), a precession period of 9000 years implies a binary separation (very roughly) on the order 10 to 100 AU, corresponding to angular separations of the order 0.1 arcsec in Orion. It should be possible to resolve separations of a few arcsec or a few tenths of an arcsec with existing or future instruments in the mid-infrared and millimetre wavelength ranges, allowing a test of the above assumptions.

Alternatively, we may simply see a poorly collimated outflow, possibly also responsible for exciting the faint features to the west of Re 50 N and SMZ 9-3, with the brighter

H_2 features only imitating a bending flow, or illuminating particular parts of a large outflow cavity. In this respect it is also interesting to note that the luminosity of the driving source L1641-S3 MMS1 is rather high ($\sim 70L_{\odot}$, compared to $\sim 5L_{\odot}$ in HH 43 MMS1), possibly suggesting that L1641-S3 MMS1 may be an intermediate-mass young stellar object. The L1641-S3 outflow may thus give further support to the suggestion that flows from intermediate- and high-mass protostars might be systematically less well collimated than those from their low-mass counterparts, as is seen e.g. in DR 21 (Davis & Smith 1996), G192.16-3.82 (Shepherd et al. 1998), the molecular outflow G75 C in the ON2 core (Shepherd et al. 1997), and HH 288 (McCaughrean & Dent, in prep.). Note however that Davis et al. (1998) find that flows from high mass protostars may nevertheless be driven by collimated jets like their low mass counterparts.

The driving source of the outflow appears to be L1641-S3 IRS = L1641-S3 MMS1. The spectral energy distribution of this source is suggestive of a Class 0 type object ($L_{\text{bol}}/L_{\text{submm}} \sim 80\text{--}90$, see Fig. 9), although its detection at the shorter IRAS wavelengths and its association with a small near-infrared nebulosity suggests that it may be approaching the Class I stage.

5. The L1641-N outflow

In Paper I, we found evidence for a large scale H_2 jet from the embedded L1641-N cluster, with the more prominent features (SMZ 23) extending to the south of the cluster. Meanwhile, a chain of optically visible Herbig-Haro objects (HH 306-

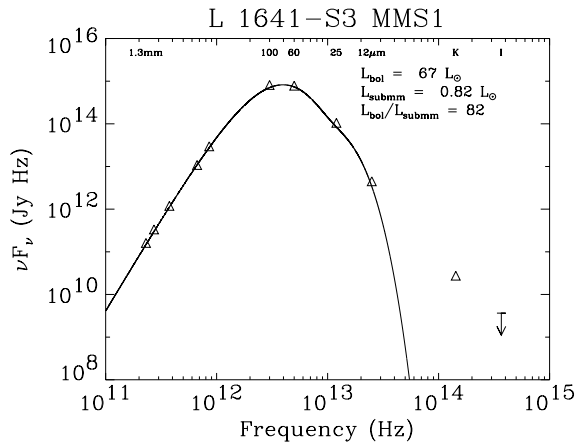


Fig. 9. Same as Fig. 5 for L1641-S3 MMS1. 1.3 mm, K-, and I-band photometry/upper limits are derived from own data, IRAS photometry is taken from the point source catalog, and additional submillimetre photometry is taken from Zavagno et al. (1997). With $L_{\text{bol}}/L_{\text{submm}} \sim 80\text{--}90$, L1641-S3 MMS1 also qualifies as Class 0 protostar.

HH 310) has been found to the north of the cluster by Reipurth et al. (1998; see also Mader et al. 1999), which is probably the counterpart to the infrared H_2 flow. However, the northern Herbig-Haro flow terminates at a distance of 6.3 pc north of the cluster, whereas the southern infrared flow as delineated mainly by SMZ 23 was seen to extend only ~ 1.8 pc south of the cluster.

In Fig. 10 we present a $2.12 \mu\text{m}$ image of the region south of the L1641-N cluster with H_2 features marked. We find a number of large H_2 features to the north-west, west, and south-west of V 380 Ori (SMZ 6-2, SMZ 6-4, and SMZ 6-16) which appear to be the continuation of the southern H_2 flow from L1641-N, beyond SMZ 23. Thus we suggest that the newly found features form the counterpart to the large northern Herbig-Haro flow. The flow heads due south at its origin in L 1641-N and then smoothly bends to the east down to SMZ 6-4. SMZ 6-16 is then located due south of SMZ 6-4, which makes its association with the flow somewhat uncertain; however, it might indicate a bending of the flow back to the original north-south direction. SMZ 6-16 has a bright rim at its southern edge and some more diffuse emission to the north, similar to SMZ 26B (HH 87/88), which is the southern terminating working surface in the HH 34 giant flow. Thus, SMZ 6-16 might indicate a large bow shock structure in a flow running from north to south. Including the newly discovered features, the southern infrared lobe of the L1641-N flow is now seen to extend over almost 30 arcmin (~ 4 pc projected length).

The region around V 380 Ori has been searched for high-velocity molecular gas by Edwards & Snell (1984) and Levreault (1988). Among other features, they found a large lobe of redshifted gas extending from about the region around V 380 Ori to the south (see also Morgan & Bally 1991; Morgan et al. 1991; flows MB 20/MB 21). No blueshifted counterflow was found. V 380 Ori was suggested as the driving source for this north-south oriented monopolar flow. In contrast, Corcoran & Ray (1995) suggested an east-west oriented outflow from V 380 Ori.

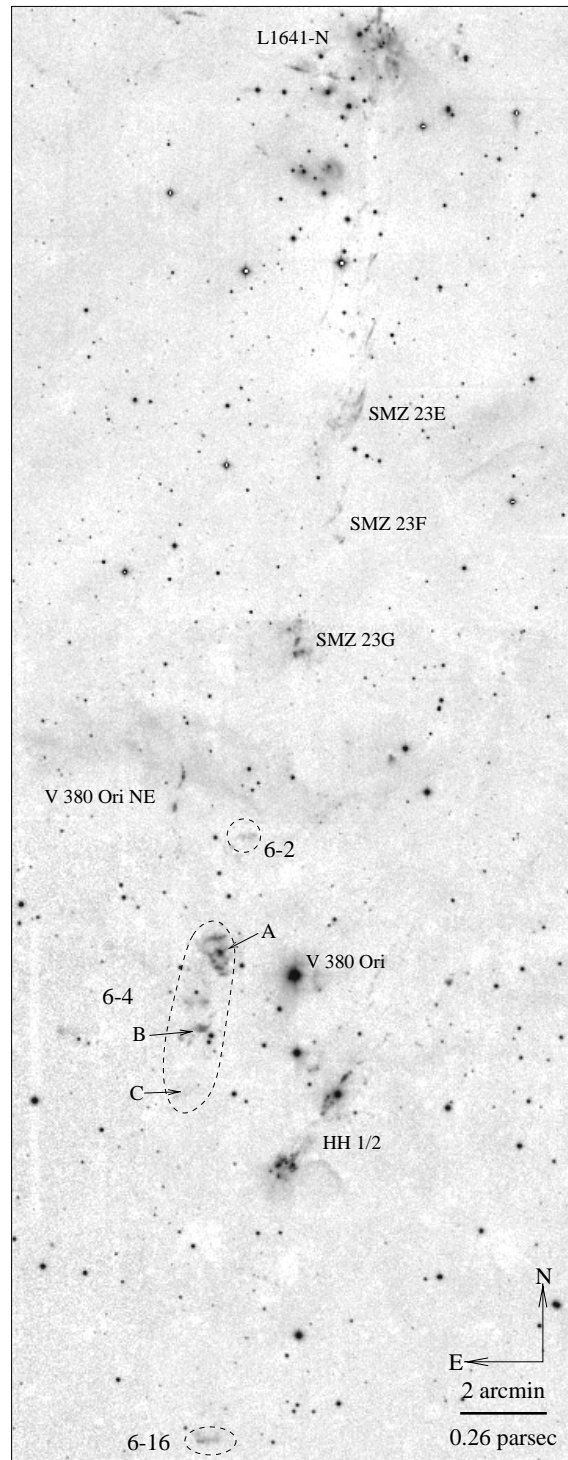


Fig. 10. $2.12 \mu\text{m}$ image of the southern lobe of the L1641-N outflow centered roughly on $\alpha = 5^{\text{h}}36^{\text{m}}26^{\text{s}}$, $\delta = -6^{\circ}37'40''$ (J2000). The image size is ~ 13 arcmin \times 33 arcmin, corresponding to ~ 1.7 pc \times 4.3 pc. H_2 features related to that flow are marked, as well as some other well known objects in the area.

The newly discovered H_2 features (including SMZ 6-16, somewhat off the track of the flow as suggested by the other H_2 features) appear superimposed on the north-south oriented red-

shifted CO outflow lobe found by Edwards & Snell (1984) and Levreault (1988). We suggest that this CO lobe is not related to V 380 Ori, but indeed another piece of the southern, redshifted part of the L1641-N outflow.

6. Summary and conclusions

Using data from our wide-field infrared imaging search for H₂ jets in the Orion A molecular cloud, we have demonstrated that parsec-scale jets can be found at infrared wavelengths. In particular, the previously known features HH 43, HH 38, and HH 64 are found to be connected by several newly discovered H₂ features into one large flow. A second large flow is found to consist of the previously known L1641-S3 CO outflow and the redshifted lobe of the L1641-S CO outflow containing HH 65. Again, the full extent of this flow is revealed by infrared imaging. In both cases, we also found deeply embedded millimetre continuum sources which we suggest to be Class 0 protostars driving the flows. Finally, we have shown that the southern lobe of the L1641-N flow, which is traced by H₂ emission, may extend over at least 4 pc, i.e. over a similar length as the northern lobe, which is traced by optically visible HH-objects. We suggest that the known molecular outflow lobe MB 20/21 (originally thought to be driven by V 380 Ori) is connected to this giant flow.

Besides the three flows discussed in this paper, other giant flows are known in Orion A. In addition to the prototype HH 34 system (Bally & Devine 1994; Eislöffel & Mundt 1997; Devine et al. 1997), the HH 1/2 system probably belongs to this class of objects (Ogura 1995). Some flows in the OMC 2/3 region also seem to extend over large distances, including the HH41/295 flow (Reipurth et al. 1997) and the H₂ flow J of Yu et al. (1997). Evidence for further large-scale flows from the L1641-N cluster is reported by Reipurth et al. (1998) and Mader et al. (1999). The discovery of so many giant flows in a single cloud appears to indicate that giant flows are not exceptionally rare systems, but may indeed be more the rule than previously thought.

The redshifted lobes of the L1641-S3 and the L1641-N flows are both seen to be associated with substantial amounts of relatively slow moving molecular gas as traced by the CO emission over most of their length. The molecular gas has probably been entrained more or less in situ, not at the base of the flows. This implies that both flows plough through the dense gas of the cloud itself, not through the rather thin medium around the cloud like most of the optically-visible giant HH flows. Thus the flows from these two protostars alone are seen to affect a significant volume of the cloud. This gives additional support to the idea that flows from young low mass stars may play an important role in the dynamical evolution of a cloud and for the regulation of star formation, not only on small scales (disruption of the cloud cores associated with the protostar driving the flow), but also on large scales (injection of momentum, excitation of turbulence, stabilisation of the cloud against collapse). However, a more complete discussion of that point is deferred to a future paper based on the complete H₂ survey for protostellar jets in Orion.

The sources of the two newly recognized giant flows, HH 43 MMS1 and L1641-S3 MMS1, are both deeply embedded, bright at 1.3 mm, very red at IRAS wavelengths, and qualify as Class 0 protostars; only one of them (L1641-S3 MMS1) appears to be associated with a small, faint near-infrared nebulosity. Similar behaviour is found for most of the Orion parsec-scale flows, implying that the most pronounced large-scale Herbig-Haro and H₂ flows are driven by very young objects, typically infrared Class I and even Class 0 type objects. Thus the largest and presumably most energetic outflows are associated with the youngest objects, not the more evolved objects like optically-visible T Tauri stars.

Acknowledgements. Many thanks are due to Frank Bertoldi, Ernst Kreysa, Karl Menten, Frédérique Motte, Bernd Weferling, and Robert Zylka for their help during the Pico Veleta observing run and first aid in reducing the 1.3 mm data. Thanks are also due to the referee, Chris Davis, for his comments which helped to strengthen some points. This work was supported by the *Deutsche Forschungsgemeinschaft, DFG* project number Zi 242/9-1.

References

- André P., Ward-Thompson D., Barsony M., 1993, *ApJ* 406, 122
 Anglada G., Rodriguez L.F., Torrelles J.M., et al., 1989, *ApJ* 341, 208
 Bally J., Devine D., 1994, *ApJ* 428, L65
 Bally J., Devine D., 1997, In: Reipurth B., Bertout C. (eds.) *Herbig-Haro Flows and the Birth of Stars*. IAU Symposium No. 182, Kluwer Academic Publishers, p. 29
 Bizenberger P., McCaughrean M.J., Birk C., Thompson D., Storz C., 1998, *Proc. SPIE* 3354, 825
 Bontemps S., André P., Terebey S., Cabrit S., 1996, *A&A* 311, 858
 Casali M.M., 1991, *MNRAS* 248, 229
 Casali M.M., 1995, *MNRAS* 277, 1385
 Chen H., Tokunaga A.T., 1994, *ApJS* 90, 149
 Chini R., Reipurth B., Sievers A., et al., 1997, *A&A* 325, 542
 Cohen M., 1990, *ApJ* 354, 701
 Cohen M., Schwartz R.D., 1983, *ApJ* 265, 877
 Cohen M., Schwartz R.D., 1987, *ApJ* 316, 311
 Cohen M., Harvey P.M., Schwartz R.D., Wilking B.A., 1984, *ApJ* 278, 671
 Cohen M., Harvey P.M., Schwartz R.D., 1985, *ApJ* 296, 633
 Colomé C., Di Francesco J., Harvey P.M., 1996, *ApJ* 461, 909
 Corcoran D., Ray T.P., 1995, *A&A* 301, 729
 Davis C.J., Smith M.D., 1996, *A&A* 310, 961
 Davis C.J., Moriarty-Schieven G., Eislöffel J., Hoare M.G., Ray T.P., 1998, *AJ* 115, 1118
 Dent W.R.F., Matthews H.E., Ward-Thompson D., 1998, *MNRAS* 301, 1049
 Devine D., Bally J., Reipurth B., Heathcote S., 1997, *AJ* 114, 2095
 Di Francesco J., Evans N.J. II, Harvey P.M., Mundy L.G., Butner H.M., 1998, *ApJ* 509, 324
 Edwards S., Snell R.L., 1983, *ApJ* 270, 605
 Edwards S., Snell R.L., 1984, *ApJ* 281, 237
 Eislöffel J., Mundt R., 1997, *AJ* 114, 280
 Elsässer H., Staude H.J., 1978, *A&A* 70, L3
 Felli M., Palagi F., Tofani G., 1992, *A&A* 255, 293
 Fendt C., Zinnecker H., 1998, *A&A* 334, 750
 Fischer O., Henning Th., Yorke H.W., 1994, *A&A* 284, 187
 Fischer O., Henning Th., Yorke H.W., 1996, *A&A* 308, 863

- Fukui Y., 1988, *Vista Astr.* 31, 217
Fukui Y., Sugitani K., Takaba H., et al., 1986, *ApJ* 311, L85
Fukui Y., Iwata T., Takaba H., et al., 1989, *Nat* 342, 161
Gredel R., 1994, *A&A* 292, 580
Haro G., 1953, *ApJ* 117, 73
Heathcote S., Morse J.A., Hartigan P., et al., 1996, *AJ* 112, 1141
Herbig G.H., 1974, *Lick Obs. Bull. No.* 658
Heyer M.H., Ladd E.F., Myers P.C., Campbell B., 1990, *AJ* 99, 1585
Hodapp K.-W., 1994, *ApJS* 94, 615
Levreault R.M., 1988, *ApJS* 67, 283
Mader S.L., Zealey W.J., Parker Q.A., Masheder M.R.W., 1999, *MNRAS* 310, 331
McCaughrean M.J., O'Dell C.R., 1996, *AJ* 111, 1977
McCaughrean M.J., Zinnecker H., Rayner J.T., 1994, *ApJ* 436, L189
McCaughrean M.J., Chen H., Bally J., et al., 1998, *ApJ* 492, L157
Moneti A., Reipurth B., 1995, *A&A* 301, 721
Morata O., Estalella R., Lopez R., Planesas P., 1997, *MNRAS* 292, 120
Morgan J.A., Bally J., 1991, *ApJ* 372, 505
Morgan J.A., Snell R.L., Strom K.M., 1990, *ApJ* 362, 274
Morgan J.A., Schloerb F.P., Snell R.L., Bally J., 1991, *ApJ* 376, 618
Ogura K., 1995, *ApJ* 450, L23
Padgett D., Brandner W., Stapelfeldt K., et al., 1999, *AJ* 117, 1490
Price S.D., Murdock T.L., Shivanandan K., 1983, *The far-infrared sky survey experiment. In: Final Report Air Force Geophysics Lab., Hanscom AFB, MA*
Reipurth B., 1985, *A&AS* 61, 319
Reipurth B., Aspin C., 1997, *AJ* 114, 2700
Reipurth B., Bally J., 1986, *Nat* 320, 336
Reipurth B., Graham J.A., 1988, *A&A* 202, 219
Reipurth B., Chini R., Krügel E., Kreysa E., Sievers A., 1993, *A&A* 273, 221
Reipurth B., Bally J., Devine D., 1997, *AJ* 114, 2708
Reipurth B., Devine D., Bally J., 1998, *AJ* 116, 1396
Schwartz R.D., Greene T.P., 1999, *AJ* 117, 456
Schwartz R.D., Cohen M., Williams P.M., 1987, *ApJ* 322, 403
Schwartz R.D., Jennings D.G., Williams P.M., Cohen M., 1988, *ApJ* 334, L99
Shepherd D.S., Churchwell E., Wilner D.J., 1997, *ApJ* 482, 355
Shepherd D.S., Watson A.M., Sargent A.I., Churchwell E., 1998, *ApJ* 507, 861
Stanke T., McCaughrean M.J., Zinnecker H., 1998, *A&A* 332, 307 (Paper I)
Stanke T., McCaughrean M.J., Zinnecker H., 1999, *A&A* 350, L43
Strom K.M., Strom S.E., 1993, *ApJ* 412, L63
Strom K.M., Strom S.E., Wolff S.C., Morgan J., Wenz M., 1986, *ApJS* 62, 39
Strom K.M., Newton G., Strom S.E., et al., 1989, *ApJS* 71, 183
Tatematsu K., Umemoto T., Kameya O., et al., 1993, *ApJ* 404, 643
Terquem C., Eislöffel J., Papaloizou J.C.B., Nelson R.P., 1999, *ApJ* 512, L131
Wilking B.A., Blackwell J.H., Mundy L.G., 1990, *AJ* 100, 758
Wouterloot J.G.A., Walmsley C.M., 1986, *A&A* 168
Wouterloot J.G.A., Walmsley C.M., Henkel C., 1988, *A&A* 203, 367
Wouterloot J.G.A., Henkel C., Walmsley C.M., 1989, *A&A* 215, 131
Yu K.C., Bally J., Devine D., 1997, *ApJ* 485, L45
Zavagno A., Molinari S., Tommasi E., Saraceno P., Griffin M., 1997, *A&A* 325, 685
Zinnecker H., Mundt R., Geballe T.R., Zealey W.J., 1989, *ApJ* 342, 337
Zinnecker H., McCaughrean M.J., Rayner J.T., 1998, *Nat* 394, 862